

The Observation of Percolation-Induced 2D Metal-Insulator Transition in a Si MOSFET

L. A. Tracy,¹ E. H. Hwang,² K. Eng,¹ G. A. Ten Eyck,¹ E. P. Nordberg,¹ K. Childs,¹ M. S. Carroll,¹ M. P. Lilly,¹ and S. Das Sarma²

¹*Sandia National Laboratories, Albuquerque, NM 87185*

²*Condensed Matter Theory Center, Department of Physics,
University of Maryland, College Park, MD 20742-4111*

(Dated: March 25, 2019)

By analyzing the temperature (T) and density (n) dependence of the measured conductivity (σ) of 2D electrons in the low density ($\sim 10^{11} \text{ cm}^{-2}$) and temperature (0.02 - 10 K) regime of a high-mobility ($\sim 15,000 \text{ cm}^2/\text{Vs}$) Si MOSFET, we establish that the putative 2D metal-insulator transition, occurring at a density $n_p \simeq 1.2 \times 10^{11} \text{ cm}^{-2}$ in our sample, is a density-inhomogeneity driven percolation transition where the density-dependent conductivity vanishes as $\sigma(n) \propto (n - n_p)^p$, with the exponent $p \simeq 1.2$ being consistent with a percolation transition. The ‘metallic’ behavior of $\sigma(T)$ for $n > n_p$ is shown to be well-described by a semi-classical Boltzmann theory, and we observe the standard weak localization-induced negative magnetoresistance behavior, as expected in a normal Fermi liquid, in the metallic phase.

PACS numbers: 71.30.+h, 73.40.-c, 73.50.Bk

The so-called two-dimensional (2D) metal-insulator transition (MIT) has been a subject [1, 2] of intense activity and considerable controversy ever since the pioneering experimental discovery [3] of the 2D MIT phenomenon in Si MOSFETs by Kravchenko and Pudalov some fifteen years ago. The apparent MIT has now been observed in almost all existing 2D semiconductor structures, including Si MOSFETs [3, 4], electrons [5, 6] and holes [7, 8] in GaAs/AlGaAs, and electrons in Si/SiGe [9, 10] systems. The basic phenomenon refers to the observation of a carrier density-induced qualitative change in the temperature dependence of the resistivity $\rho(n, T)$, where n_c is a critical density separating an effective ‘metallic’ phase ($n > n_c$) from an ‘insulating’ phase ($n < n_c$), exhibiting $d\rho/dT > 0$ (< 0) behavior typical of a metal (insulator).

The excitement and controversy in the subject arise from the deep conceptual questions associated with the nature of the MIT and the metallic phase. In particular, it is theoretically well-established [1] that a non-interacting (or weakly interacting) disordered 2D electron system is an insulator at $T = 0$, and therefore it follows [1] that if the 2D MIT is a true $T = 0$ quantum phase transition (QPT), then the 2D metallic phase, if it survives all the way to $T = 0$, must necessarily be a novel and exotic non-Fermi liquid phase since it cannot be connected adiabatically to the non-interacting 2D electron system, which is always localized in the presence of any disorder. The alternative possibility [2] is that the metallic phase is allowed only at finite temperatures, and the 2D MIT is not a QPT, but a density-induced crossover from a weakly localized ‘effective’ metallic phase to a strongly localized insulator. These two qualitatively distinct viewpoints (i.e. QPT [1] versus crossover [2]) have both received support in the literature, and experimental results have been presented claiming support for the

QPT [11] and the finite-temperature crossover [6, 8] viewpoints, respectively. Whether the observed 2D MIT is a novel ($T = 0$) QPT leading to an exotic 2D non-Fermi liquid metallic phase established by interaction effects or is a finite-temperature crossover between an effective metallic phase and the insulating phase is obviously a question of great fundamental importance.

In this Letter, we provide the first experimental evidence that the 2D MIT in the Si MOSFET system is a finite-temperature, density inhomogeneity driven semi-classical percolation transition, and is therefore not a QPT. The 2D MIT in high-mobility GaAs electron and hole systems [6, 8, 12] has already been experimentally demonstrated to be a percolation transition, but our work provides the first compelling evidence supporting the percolation scenario in Si MOSFETs. We also establish that the metallic phase is a conventional Fermi liquid by showing that (1) the measured transport properties in the effective metallic phase qualitatively agree very well with the conclusions of a semi-classical Boltzmann transport theory [13] taking into account the detailed density and temperature dependence of carrier screening properties, and (2) the expected negative magnetoresistance signature of the conventional weak localization behavior [14] is clearly manifest experimentally in the effective metallic phase of our samples.

The two samples used in this study are Si MOSFET structures with a peak mobility of $\sim 1.5 \times 10^4 \text{ cm}^2/\text{Vs}$ (sample A) and $\sim 1 \times 10^4 \text{ cm}^2/\text{Vs}$ (sample B). For both samples, the 2D electron gas (2DEG) resides at the Si-SiO₂ gate oxide interface, where the SiO₂ thickness is nominally 35 nm for sample A and 10 nm for sample B. Ohmic contacts to the 2DEG consist of n⁺ Si regions formed by implantation of As and an n⁺ polySi gate is used to induce carriers. The 2DEG resistivity is exper-

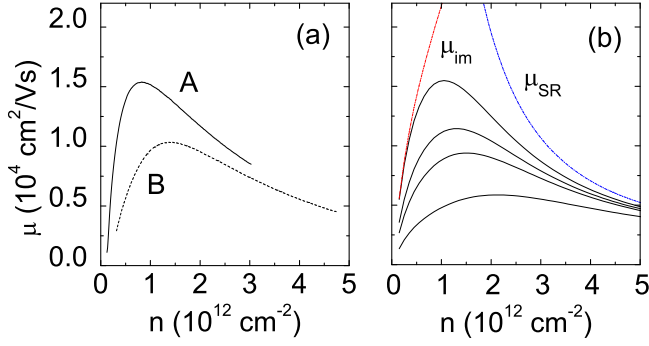


FIG. 1: (color online) (a) Experimental mobility μ as a function of density n for two samples, A and B, at a temperature $T = 0.25 \text{ K}$. (b) Theoretical mobility as a function of density. High (low) density mobility is limited by the surface roughness μ_{SR} (charged impurity μ_{im}) scattering. Different curves correspond to different charged impurity densities ($n_i = 6, 9, 12$, and $24 \times 10^{10} \text{ cm}^{-2}$ from top to bottom), but with the same surface roughness ($\Delta = 1.9 \text{ \AA}$, $\Lambda = 26 \text{ \AA}$).

imentally determined via standard four-terminal lock-in measurements and the density is calibrated via measurements of the Hall resistivity.

In Fig. 1 we show the density-dependent mobility of samples A and B along with the theoretically calculated mobility curves. Our theoretical calculations [15], which include the temperature-dependent finite wavevector screening of the charged impurity Coulomb scattering, capture the essential qualitative features of the data. The mobility (μ) first rises steeply with density (n) reaching a maximum at a characteristic density n_m , beyond which μ falls off slowly with increasing n , reaching essentially a sample-independent high-density (for $n \gg n_m$) value of roughly $\mu \sim 3 \times 10^3 \text{ cm}^2/\text{Vs}$. It is well-known [16] that the high-density mobility is determined by the short-range surface roughness scattering at the Si-SiO₂ interface. At low carrier densities ($n < 10^{12} \text{ cm}^{-2}$) however, long-range Coulomb scattering by unintentional random charged impurities invariably present on the insulating oxide side of the Si-SiO₂ interface dominates the 2D mobility, and, as has been emphasized [17] in the literature, all Si 2D MIT behavior manifests itself at low carrier densities ($n \sim 10^{11} \text{ cm}^{-2}$) where the charged impurity scattering dominates transport and the short-range interface roughness scattering is negligible. We emphasize the fact that the 2D MIT phenomenon (i.e. the critical density for the insulator-to-metal transition and the density range for the ‘anomalous’ metallic phase with a strongly temperature dependent 2D resistivity) occurs in the density regime $n \sim 10^{11} \text{ cm}^{-2}$ which, being substantially below n_m , is completely dominated by screened Coulomb scattering. This dominance of Coulomb scattering in the 2D MIT physics is crucial for the percolation physics which arises from the nonlinear failure of screening of the long-range coulombic charged

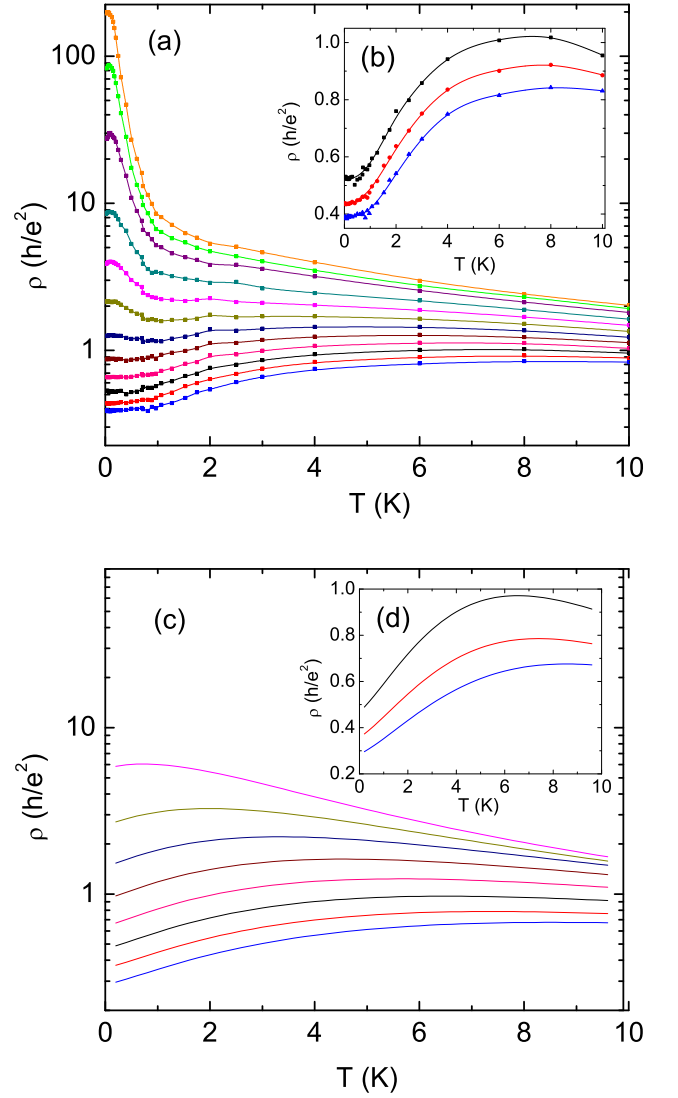


FIG. 2: (color online) (a) Experimental resistivity ρ in units of h/e^2 as a function of temperature for sample A at 2D electron densities (from top to bottom) $n = 1.07, 1.10, 1.13, 1.20, 1.26, 1.32, 1.38, 1.44, 1.50, 1.56, 1.62$, and $1.68 \times 10^{11} \text{ cm}^{-2}$. Inset (b) Enlarged view of data in the effective metallic regime at $n = 1.56, 1.62$, and $1.68 \times 10^{11} \text{ cm}^{-2}$. Solid lines are guides to the eye. (Data below 0.1 K may not be reliable due to electron heating.) (c) Theoretically calculated temperature and density dependent resistivity for sample A for densities $n = 1.26, 1.32, 1.38, 1.44, 1.50, 1.56, 1.62$, and $1.68 \times 10^{11} \text{ cm}^{-2}$ (from top to bottom). Inset shows the resistivities for $n = 1.56, 1.62$, and $1.68 \times 10^{11} \text{ cm}^{-2}$.

impurity potential, to be discussed below.

In Fig. 2 we show our measured (Fig. 2(a) - (b)) and calculated (Fig. 2(c) - (d)) temperature and density dependent resistivity ($\rho(T, n)$) for sample A with the maximum mobility of $1.5 \times 10^4 \text{ cm}^2/\text{Vs}$ (see Fig. 1(a)). The results for sample B are similar, but with a larger value of the critical density, $n_c \sim 2.5 \times 10^{11} \text{ cm}^{-2}$ (and somewhat weaker temperature dependence), con-

sistent with its lower peak mobility $\sim 1 \times 10^4 \text{ cm}^2/\text{Vs}$. The classic 2D MIT behavior is apparent in Fig. 2(a) where $\rho(T)$ for various densities manifests the clear distinction between metallic ($d\rho/dT > 0$) and insulating ($d\rho/dT < 0$) behavior separated (visually) by a critical density $n_c \sim 1.4 \times 10^{11} \text{ cm}^{-2}$. We note that the temperatures quoted in Fig. 2a and b are those of the cryostat cold finger; although the resistivity continues to evolve below $T \sim 100 \text{ mK}$ (albeit slowly), we cannot claim in this regime ($T < 100 \text{ mK}$) that the 2D electrons and cold finger are in thermal equilibrium down to the base temperature of our cryostat (20 mK). The inset, Fig. 2(b) shows in detail the metallic behavior for $n > n_c$, which manifests more than a factor of 2 increase in $\rho(T)$ for $T \sim 0.1 - 7 \text{ K}$ before decreasing slightly at higher temperatures. The strong initial increase in $\rho(T)$ with T arises [13] from the temperature-induced weakening of screening at these low densities as T/T_F increases from 0.01 at low temperatures essentially to 1 at $T \sim 8 \text{ K}$ since $T_F \approx 7.3 \text{ K}$ for $n = 10^{11} \text{ cm}^{-2}$. (Phonon scattering is unimportant in Si MOSFET for $T < 10 - 20 \text{ K}$.)

Finally, in Fig. 2(c) we show our theoretically calculated $\rho(T, n)$ where the Boltzmann transport is calculated using the screened charged impurity scattering as the only resistive scattering mechanism [13]. We note that the basic features of the experimental metallic phase are qualitatively well-captured by the screening theory with $\rho(T)$ rising approximately by a factor of 2 initially and then decreasing slightly at higher (lower) temperatures (densities) around $T/T_F \gtrsim 1$ due to quantum-classical crossover [13]. The theoretical results, following the work of Ref. [13], are being shown here in order to demonstrate that a realistic semiclassical transport theory including the screened long-range scattering by charged impurities completely captures all the qualitative aspects of the experimental results with the basic physics being a strong temperature and density dependent modification in the effective screened disorder due to the large change in the effective T/T_F in the experimental $T \sim 0.1 - 10 \text{ K}$ temperature range. We point out that, by definition, the theoretical transport results in Figs. 2(c) and (d) apply only in the metallic regime since the metal-insulator transition cannot be captured in a Boltzmann theory.

Having established the phenomenology of the 2D MIT behavior in Fig. 2, we now come to the nature of the density driven transition itself. We plot in Fig. 3 our measured conductivity $\sigma(n)$ as a function of n to see if a percolation behavior, $\sigma(n) \sim (n - n_p)^p$, where n_p , p are the percolation transition density and exponent respectively, is manifested near the MIT point (i.e. around n_c , where $d\rho/dT$ changes its sign in Fig. 2(a)). Our regression analysis leads to an excellent fit to the percolation formula with $p \approx 1.2 \pm 0.1$ and $n_p \approx 1.2 \times 10^{11} \text{ cm}^{-2}$. The fit describes $\sigma(n)$ well over two orders of magnitude change in conductivity. The fact that our best fit values of n_p and p are almost independent of temperature at low

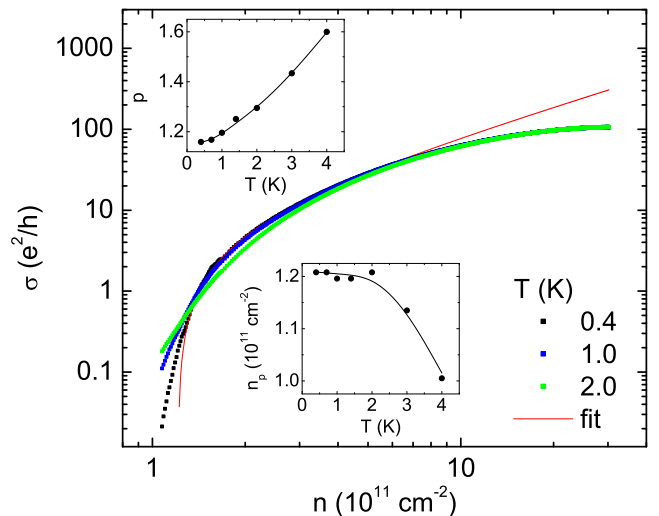


FIG. 3: (color online) (a) Main plot: Points show experimental conductivity σ in units of e^2/h versus electron density n at three temperatures, $T = 0.4, 1.0$, and 2.0 K for sample A. The solid line is a fit to the $T = 0.4 \text{ K}$ data of the form $\sigma = A(n - n_c)^p$. The upper and lower insets show the exponent p and critical density n_c , respectively, as a function of temperature. Solid lines are a guide to the eye.

temperatures is a good indicator for the percolation transition being the correct description for the 2D MIT phenomenon shown in Fig. 2. We also note that the percolation transition density $n_p \sim 1.2 \times 10^{11} \text{ cm}^{-2}$ is somewhat lower than the nominal ‘critical’ density $n_c \sim 1.4 \times 10^{11} \text{ cm}^{-2}$ in Fig. 2(a). This slight inconsistency between n_p and n_c (i.e. $n_p \lesssim n_c$) has been observed for 2D electrons [6] and holes [8] in high-mobility GaAs/AlGaAs heterostructures. This arises from the non-uniqueness of n_c in the sense that n_c is in fact somewhat temperature dependent, as was originally pointed out [18] rather early in the literature.

In Fig. 4 we show our observed weak localization behavior by plotting the expected [14] negative magnetoresistance in the metallic phase as a function of an applied weak magnetic field. The weak localization data in Fig. 4 is fitted to the standard di-gamma function behavior expected of a disordered 2D system[14]

$$\Delta\sigma = -\alpha \frac{e^2}{h} \frac{g_v}{\pi} \left[\Psi\left(\frac{1}{2} + \frac{\tau_B}{\tau}\right) - \Psi\left(\frac{1}{2} + \frac{\tau_B}{\tau_\phi}\right) \right], \quad (1)$$

where $\tau_B \equiv \hbar/4eB_\perp D$ and D is the diffusion coefficient. The behavior is quite normal, explicitly demonstrating that our observed metallic phase ($n > n_c, n_p$) is indeed the usual weakly localized Fermi liquid metallic phase, and not some exotic non-Fermi liquid $T = 0$ metal. The observation of the expected weak localization behavior in the 2D metallic phase along with the percolative nature of the transition is strong evidence that the experimental 2D MIT is not a QPT, but a crossover.

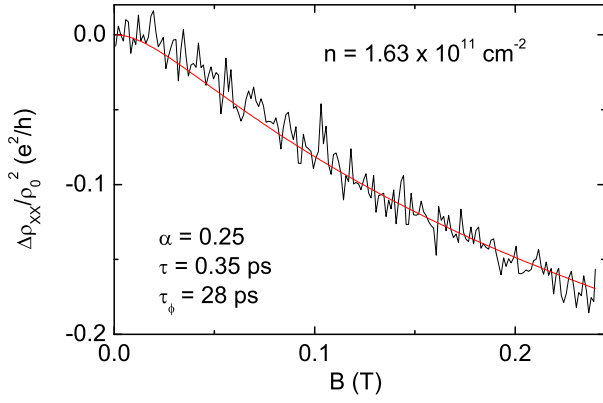


FIG. 4: (color online) Measured weak localization correction to the resistivity, $\Delta\rho_{xx}/\rho_0^2$ in units of e^2/h versus perpendicular magnetic field B at a density $n = 1.63 \times 10^{11} \text{ cm}^{-2}$ at $T = 100 \text{ mK}$. The red line is a fit to the standard weak localization correction (see text). The momentum relaxation time τ is determined from the mobility, while the weak localization fit yields a correction amplitude $\alpha = 0.25$ and phase relaxation time $\tau_\phi = 28 \text{ ps}$.

Before concluding, we briefly discuss the physics underlying the percolation transition. As emphasized earlier in this Letter, the 2D MIT phenomenon occurs in the transport regime dominated by long-range Coulombic charged impurity scattering. It was pointed out some years ago [19] that such a transport regime is susceptible at low carrier densities to a semiclassical percolation MIT since large scale density inhomogeneities (i.e. puddles) could appear in the system due to the nonlinear failure of screening of the charged impurities at low carrier densities. One can approximately estimate [19] the percolation transition density, n_p , by considering the inhomogeneous density fluctuations in the system, leading to $n_p \sim 0.2\sqrt{n_i}/d$, where n_i is the effective 2D charged scatterer density and d is the effective separation between the 2D carriers and the scatterers. Using $n_i = 6 \times 10^{10} \text{ cm}^{-2}$, the value needed to get the correct mobility at higher densities (This value of n_i is roughly consistent with C-V measurements which estimate the density of fixed charge near the Si-SiO₂ interface to be $\sim 8 \times 10^{10} \text{ cm}^{-2}$), and taking $d \sim 5 - 6 \text{ nm}$, which is consistent with the 2D electron layer in the Si MOSFET being about 5 nm away from the interface due to the self-consistent potential produced by the electrons themselves, we get $n_p \sim 1 \times 10^{11} \text{ cm}^{-2}$ for our sample A, which is close to our experimentally extracted percolation density in Fig. 3(a). (We note that d corresponds to the effective separation between the 2D electrons and the charged impurities, which must incorporate the fact that the 2D electrons are on the average about 5 nm inside Si at $n \sim 10^{11} \text{ cm}^{-2}$.) The 2D conductivity percolation exponent is numerically known to be around 1.31, which is close to the exponent value 1.2 ± 0.1 we get in our analysis. Finally, we note that

the puddles produced by the nonlinear failure of screening of charged impurities in low-density 2D systems have been directly observed in 2D GaAs [20] and graphene [21] systems.

In conclusion, we have experimentally established that the 2D MIT in Si MOSFETs is a percolation-induced transition driven by the dominance of the long-range charged impurity disorder. At low carrier densities, the failure of linear screening leads to the formation of inhomogeneous puddles in the 2D density landscape, which then produces a semi-classical percolation transition. The nature of the percolation transition and the effective metallic phase is the same in Si MOSFETs and 2D GaAs electron [6] and hole [8] systems. The metallic temperature dependence arises from the strong temperature dependence of screening and the percolation transition arises from the low-density failure of screening. The 2D MIT is therefore a quantum crossover phenomenon, not a QPT, from an effective (weakly localized) metallic phase to a strongly localized insulating phase. We have also shown explicitly that the metallic phase manifests the conventional weak localization behavior as expected of a disordered Fermi liquid.

This work was performed, in part, at the Center for Integrated Nanotechnologies, a U.S. DOE, Office of Basic Energy Sciences user facility. Sandia National Laboratories is a multi-program laboratory operated by Sandia Corporation, a Lockheed-Martin Company, for the U. S. Department of Energy under Contract No. DE-AC04-94AL85000.

-
- [1] S. V. Kravchenko and M. P. Sarachik, Rep. Prog. Phys. **67**, 1 (2004); E. Abrahams, S. V. Kravchenko, and M. P. Sarachik, Rev. Mod. Phys. **73**, 251 (2001).
 - [2] S. Das Sarma and E. H. Hwang, Solid State Commun. **135**, 579 (2005).
 - [3] S. V. Kravchenko et al., Phys. Rev. B **50**, 8039 (1994).
 - [4] S. V. Kravchenko et al., Phys. Rev. B **51**, 7038 (1995).
 - [5] M. P. Lilly et al., Phys. Rev. Lett. **90**, 056806 (2003).
 - [6] S. Das Sarma et al., Phys. Rev. Lett. **94**, 136401 (2005).
 - [7] A. P. Mills et al., Phys. Rev. Lett. **83**, 2805 (1999).
 - [8] M. J. Manfra et al., Phys. Rev. Lett. **99**, 236402 (2007).
 - [9] K. Lai et al., Phys. Rev. B. **72**, 081313 (2005).
 - [10] K. Lai et al., Phys. Rev. B. **75**, 033314 (2007).
 - [11] S. Anissimova et al., Nat. Phys. **3**, 707 (2007).
 - [12] R. Leturcq et al., Phys. Rev. Lett. **90**, 076402 (2003); Y. Meir, Phys. Rev. Lett. **83**, 3506 (1999); G. Allison et al., Phys. Rev. Lett. **96**, 216407 (2006); L. A. Tracy et al., Solid State Commun. **137**, 150 (2006); Y. Hanein et al., Phys. Rev. B **58**, R7520 (1998).
 - [13] S. Das Sarma and E. H. Hwang, Phys. Rev. Lett. **83**, 164 (1999); Phys. Rev. B **69**, 195305 (2004).
 - [14] P. A. Lee and T. V. Ramakrishnan, Rev. Mod. Phys. **57**, 287 (1985); S. Hikami, A. Larkin, and Y. Nagaoka, Prog. Theor. Phys. **63**, 707 (1980).
 - [15] All calculations are carried out following the prescrip-

- tion described in refs. 13 above, where all the theoretical details are available.
- [16] T. Ando, A. B. Fowler, and F. Stern, *Rev. Mod. Phys.* **54**, 438 (1982).
 - [17] T. M. Klapwijk and S. Das Sarma, *Solid State Commun.* **110**, 581 (1999).
 - [18] J. Yoon *et al.*, *Phys. Rev. Lett.* **82**, 1744 (1998).
 - [19] A. L. Efros, *Solid State Commun.* **65**, 1281; **70**, 253 (1989); S. He and X. C. Xie, *Phys. Rev. Lett.* **80**, 3324 (1998); J. A. Nixon and J. Davies, *Phys. Rev. B* **41**, 7929 (1990); A. L. Efros *et al.*, *Phys. Rev. B* **47**, 2233 (1993); J. Shi and X. C. Xie, *Phys. Rev. Lett.* **88**, 086401 (2002).
 - [20] S. Ilani *et al.*, *Phys. Rev. Lett.* **84**, 3133 (2000).
 - [21] J. Martin *et al.*, *Nat. Phys.* **4**, 144 (2008).